



Buckling Analysis of Composite Plates under Thermal and Mechanical Loading

Prof. Dr. Adnan Naji Jameel Dr. Ibtehal Abbas Sadiq M.Sc. student Hasanain Ibraheem Nsaif

ebtihalabas@yahoo.com

Univ. of Baghdad / Mech. Eng. Dept., Baghdad-Iraq

Abstract

Buckling analysis of composite laminates for critical thermal (uniform and linear) and mechanical loads is reported here. The objective of this work is to carry out theoretical investigation of buckling analysis of composite plates under thermo-mechanical loads, and experimental investigation under mechanical loads. The analytical investigation involved certain mathematical preliminaries, a study of equations of orthotropic elasticity for classical laminated plate theory (CLPT), higher order shear deformation plate theory (HSDT), and numerical analysis (Finite element method), then the equation of motion are derived and solved using Navier method and Levy method for symmetric and anti-symmetric cross-ply and angle-ply laminated plates to obtain buckling load by solving eigenvalue problem for different boundary conditions under different thermo-mechanical loading. It also contained a verification study of these methods with those published by other researchers. The results obtained gives good agreement which shows that maximum percentage discrepancy was 7.6152 %. The experimental investigation is to find mechanical properties at room temperature of glass-polyester such as longitudinal, transverse and shear modulus under tension test. Also, to find critical load that cause buckling under buckling test. Analytical and numerical results of critical buckling load studied the effect of Boundary conditions, No. of layers, No. of half wavelengths in y-direction, lamination angle, aspect ratio, and thickness ratio on buckling load under different thermo-mechanical loading condition.

Keyword: thermal load, buckling analysis, composite plates, thermo-mechanical load, mechanical load, finite element

تحليل الانبعاج للصفائح المركبة تحت تأثير الأحمال الحرارية والميكانيكية

الخلاصة :

يتضمن البحث دراسة وتحليل الانبعاج للصفائح المواد المركبة المعرضة للأحمال الحرارية (المنتظمة والخطية) والميكانيكية نظريا وتحليل الانبعاج لتلك الصفائح وعمليا. في الجانب النظري تم دراسة معادلات الحركة عن النظرية الكلاسيكية CLPT وعن نظرية اجهاد القص ذات الرتبة العالية HSDT وتم اشتقاق هذه المعادلات وحلها تحليليا باستخدام طريقة نافير وطريقة ليفي لجميع انواع الاسناد للصفائح المركبة المتماثلة وغير المتماثلة مع الاخذ بنظر الاعتبار نسبة طول الى عرض الصفيحة ، عدد الطبقات ، زاوية دوران

الياف الطبقات ، ونسبة نحافة الطبقات وتأثيرها على الحمل الحرج المسبب في تأثير الانبعاج بحل مسألة Eigenvalue للاحمال الحرارية والميكانيكية ، وايضا تم تحليل حمل الانبعاج الحرج عدديا بأستخدام طريقة العناصر المحددة. يتضمن الجانب العملي حساب الخواص الميكانيكية (ضمن درجة حرارة الغرفة) لمادة الفايبر كلاس – بوليستر عن طريق اختبار الشد وايجاد حمل الانبعاج الحرج بواسطة اختبار الانبعاج. النتائج التي تم الحصول عليها اعطت موافقة جيدة مع النتائج المنشورة لباحثين اخرين.

Introduction

Fiber-reinforced composites are used extensively in the form of relatively plate, and consequently the load carrying capability of composite plate against buckling has been intensively considered by researchers under various loading and boundary conditions. Thus far, there have been numerous studies on composite laminated structures which find widespread applications in many engineering fields namely aerospace, biomedical, civil, marine and mechanical engineering because of their ease of handling, good mechanical properties and low fabrication cost. They also possess excellent damage tolerance and impact resistance. The initial theoretical research into buckling analysis was Gossard et al. 1952[1] outlined an approximate method (Ritz method) based on von Karman large-deflection plate theory for calculating the deflections of flat plates subjected to thermal buckling theoretically and experimentally. This method is used to determine the deflections of a simply supported plate subjected to a temperature distribution over the plate surface. Sharma et al. 1980[2] studied the uniaxial compressive buckling response of arbitrary laminated composite plates of anti-symmetric cross-ply and angle-ply laminates for two boundary conditions (SCSC, SCSF). The differential equation governing the elastic response materials have developed using CLPT (classical laminated plate theory) that solved by using Levy method (direct

Integration). The effect of aspect ratio, lamination angle on buckling behavior has been studied. Thangaratnam K. R. et al. 1988[3] studied buckling analysis of composite laminates for critical temperature under thermal load based on finite element method using semi-loof element. Results are presented for cross-ply and angle-ply laminates for simply supported, clamped and combined of them with varying ratio for coefficient of thermal expansion and different No. of layers. Liangxin S. and Zhiyu S. 1992[4] investigated bending deflection, buckling load and natural frequency for symmetric cross-ply simply supported laminated plates using Navier solution based on HSPT and Finite element method for different thickness ratio. Kam T. Y. and Chang R. R. 1993[5] studied optimal ply orientation and No. of layers of thick laminated composite plates for max. uniaxial buckling load and vibration frequency based on finite element using global optimization technique for cases of symmetric and anti-symmetric angle-ply simply supported laminated composite plates with various material properties, side to thickness ratio (b/h), aspect ratio (a/b), and different No. of layers. Prabhu M.R. and Dhanaraj R. 1994[6] analyzed thermal buckling of laminated composite plate using finite element method. Nine node elements is employed for thermal buckling analysis of symmetric cross-ply and angle-ply laminates subjected to uniform temperature distribution. The effects of modulus ratio, length to thickness ratio, fiber orientation, aspect ratio and various



boundary conditions (SSSS, CCCC) on the critical temperature are analyzed. Argyris J. and Tenek L. 1994[7], in this study, the behavior of simply supported isotropic and thin laminated composite plates under thermal loads have examined for bending, buckling and post-buckling of symmetric angle-ply square laminates. The material properties are assumed to be independent on temperature. Finite element using triangular shell element contains 3 nodes has been implemented. Ghosh A. K. and Dey S. K. 1994[8] studied buckling analysis of simply supported cross-ply laminated square plates based on finite element using four nodes with seven degree of freedom at each node for thick and thin laminated plates for different aspect ratio, modulus ratio under uniaxial loading conditions. Sun L. and Xiaoping S. 1994[9], developed higher order displacement field for the analysis of the thermo-mechanical buckling of composite plates subjected to thermal or mechanical load. Exact closed-form solutions of symmetric cross-ply laminates are obtained using Navier method including effects of transverse shear deformation on critical temperature and critical load. The effects played with side to thickness ratio, coefficients of thermal expansion ratio and different No. of layers. Simelane S. P. 1998 [10] studied thermal buckling of laminated composite plate using finite element computer package ABAQUS with five degrees of freedom in each node. The effects of lamination angle, modulus ratio, plate aspect ratio, and boundary constraints upon the critical buckling load temperature were investigated. Matsunaga H. 2005[11] presented higher order deformation theory for thermal buckling load of cross-ply laminated composite and sandwich

square plates by using Navier method which can take into account the effects of transverse shear stress of simply supports multilayered plate. Shariyat M. 2007[12] investigated thermal buckling analysis of rectangular composite plates under uniform temperature rise based on layerwise plate theory and determine the buckling temperature using Budiansky instability criterion in a computerized solution. The effects played with boundary conditions (SSSS, CCCC) and various geometric by assuming that material property is to be vary with temperature. Yu L. H. and Wang C. Y. 2008[13] studied the buckling of a rectangular plate based on an elastic foundation. Two opposite sides are simply supported and other two edges is to be (SS and CC), and Levy method (direct integration method) is used based on classical plate theory for different aspect ratio. The plate is subjected to uniaxial and biaxial compressive load. Ozben T. 2009[14] studied the critical uniaxial buckling load using finite element and Ritz methods for different plate dimensions ratio and different orientation angles with symmetric and anti-symmetric laminated plates for (SSSS, SSSC and SCSC). Rajesh et al. 2009[15] examined the random system properties on thermal buckling load of laminated composite plates under uniform temperature rise using finite element for deriving the eigenvalue problem with and without temperature dependent elastic properties. Numerical results present that the characteristics of thermal buckling load of the plate are influence by (SSSS, CCCC and SCSC), plate thickness ratio, aspects ratio. The random system properties having random change in all input material variables, thermal expansion coefficients and plate

thickness. Shiau et al. 2010[16] studied thermal buckling behavior of composite laminated plates using finite element method for cross-ply and angle-ply laminates with various degree of orthotropy, fiber angle, aspect ratio, different boundary conditions and No. of layers.

From above literature review, there are a few literatures available in thermo-mechanical field. In the present work, thermo-mechanical buckling analysis of shear deformable laminated plates with thermo-elastic properties has investigated analytically. In the present study, the temperature distribution field is assumed to be uniform and linear through the plate thickness. Thermal expansion coefficients and elastic constants is assumed to be independent of temperature. The formulations are based on Reddy's higher order shear deformation plate theory and classical laminated plate theory. Navier method of higher order shear deformation theory, Levy method of classical laminated plate theory and Finite element coded by ANSYS 13.0 is used to formulate numerical model. Many design parameters are changed to study their effects on the buckling characteristics such as No. of cross-ply and angle-ply layers, aspect ratio (a/b), thickness ratio (a/h), type of boundary conditions and number of half wavelengths.

Theoretical Analysis

A. Classical Laminated Plate Theory (Clpt)

Displacement

The displacement field of CLPT contains only three dependent variables [17]:

$$u(x,y) = u_0(x,y) + z\bar{Q}_x(x,y) \quad (1 a)$$

$$v(x,y) = v_0(x,y) + z\bar{Q}_y(x,y) \quad (1 b)$$

$$w(x,y) = w_0(x,y) \quad (1 c)$$

where: \bar{Q}_x , \bar{Q}_y denote rotations about y and x axes respectively, and

u_0 , v_0 , w_0 denote the displacement components along (x,y,z) directions respectively of a point on the mid-plane (i.e....z=0).

Stress and Strain

The total strains can be written as follows:

$$\begin{Bmatrix} \epsilon_{xx} \\ \epsilon_{yy} \\ \gamma_{xy} \end{Bmatrix} = \begin{Bmatrix} \epsilon_{xx}^{(0)} \\ \epsilon_{yy}^{(0)} \\ \gamma_{xy}^{(0)} \end{Bmatrix} + z \begin{Bmatrix} \epsilon_{xx}^{(1)} \\ \epsilon_{yy}^{(1)} \\ \gamma_{xy}^{(1)} \end{Bmatrix} = \begin{Bmatrix} \frac{\partial u_0}{\partial x} - \alpha_x T_0 \\ \frac{\partial v_0}{\partial y} - \alpha_y T_0 \\ \frac{\partial u_0}{\partial y} + \frac{\partial v_0}{\partial x} - \alpha_{xy} T_0 \end{Bmatrix} + z \begin{Bmatrix} \frac{\partial \bar{Q}_x}{\partial x} - \alpha_x T_1 \\ \frac{\partial \bar{Q}_y}{\partial y} - \alpha_y T_1 \\ \frac{\partial \bar{Q}_x}{\partial y} + \frac{\partial \bar{Q}_y}{\partial x} - \alpha_{xy} T_1 \end{Bmatrix} \quad (2)$$

The transformed stress-strain relations of an orthotropic lamina in a plane state of stress are; for \bar{Q}_{ij} , see [17]:

$$\begin{Bmatrix} \sigma_x \\ \sigma_y \\ \sigma_{xy} \end{Bmatrix}_k = \begin{bmatrix} \bar{Q}_{11} & \bar{Q}_{12} & \bar{Q}_{16} \\ \bar{Q}_{12} & \bar{Q}_{22} & \bar{Q}_{26} \\ \bar{Q}_{16} & \bar{Q}_{26} & \bar{Q}_{66} \end{bmatrix}_k \begin{Bmatrix} \epsilon_{xx} - \alpha_x \Delta T \\ \epsilon_{yy} - \alpha_y \Delta T \\ \gamma_{xy} - 2\alpha_{xy} \Delta T \end{Bmatrix} \quad (3)$$

Equation of Motion

The Euler-Lagrange equations are obtained by setting the coefficient of δu_0 , δv_0 , δw_0 to zero separately [17]:

$$\delta u_0: \frac{\partial N_{xx}}{\partial x} + \frac{\partial N_{xy}}{\partial y} = 0 \quad (4 a)$$

$$\delta v_0: \frac{\partial N_{xy}}{\partial x} + \frac{\partial N_{yy}}{\partial y} = 0 \quad (4 b)$$

$$\delta w_0: \frac{\partial^2 M_{xx}}{\partial x^2} + 2 \frac{\partial^2 M_{xy}}{\partial x \partial y} + \frac{\partial^2 M_{yy}}{\partial y^2} + \hat{N}_{xx} \frac{\partial^2 w}{\partial x^2} + \hat{N}_{yy} \frac{\partial^2 w}{\partial y^2} = 0 \quad (4 c)$$

Levy Method

Levy method, can be used to solve the governing equations of various laminated plates for which two (parallel) opposite edges are simply supported and the other two edges can have any boundary conditions.

For cross-ply rectangular laminates with edges $y=0$ and $y=b$ simply supported and the other two edges $x=\pm a/2$, having arbitrary boundary conditions. Assume the following representation of the displacement [17]:

$$u_0(x,y,t) = \sum_{m=1}^{\infty} U_m(x) \sin \beta y \dots \quad (5 a)$$

$$v_0(x,y,t) = \sum_{m=1}^{\infty} V_m(x) \cos \beta y \quad (5 b)$$

$$w_0(x,y,t) = \sum_{m=1}^{\infty} W_m(x) \sin \beta y \quad (5 c)$$

Where: $\beta = \frac{n\pi}{b}$; $U_m(x)$, $V_m(x)$, $W_m(x)$ are independent of y (function of x).

n = No. of half wavelengths in y -direction ($n=1, 2, 3$)

b = Length of the plate along y -direction.

For angle-ply rectangular laminates with edges $x=0$ and $x=a$ simply supported and the other two edges $y=\pm b/2$, having arbitrary boundary conditions. Assume the following representation of the displacement [17]:

$$u_0(x,y,t) = \sum_{m=1}^{\infty} U_m(y) \sin \alpha x \quad (6 a)$$

$$v_0(x,y,t) = \sum_{m=1}^{\infty} V_m(y) \cos \alpha x \quad (6 b)$$

$$w_0(x,y,t) = \sum_{m=1}^{\infty} W_m(y) \sin \alpha x \quad (6 c)$$

Where: $\alpha = \frac{m\pi}{a}$; a = Width of the plate along x -direction.

m = No. of half wavelengths in x -direction ($m= 1, 2, 3$)

B. Third Order Shear Deformation Plate Theory (Tsdt)

Displacement

The displacement field of (HSST) is of the form [17]:

$$u(x,y,z,t) = u_0(x,y,t) + z\phi_x(x,y,t) - \frac{4}{3h^2} z^3 \left(\phi_x + \frac{\partial w_0}{\partial x} \right) \quad (7 a)$$

$$v(x,y,z,t) = v_0(x,y,t) + z\phi_y(x,y,t) - \frac{4}{3h^2} z^3 \left(\phi_y + \frac{\partial w_0}{\partial y} \right) \quad (7 b)$$

$$w(x,y,z,t) = w_0(x,y,t) \quad (7 c)$$

Stress And Strain

The total strains can be written as follows [17]:

$$\begin{Bmatrix} \epsilon_{xx} \\ \epsilon_{yy} \\ \gamma_{xy} \end{Bmatrix} = \begin{Bmatrix} \epsilon_{xx}^{(0)} \\ \epsilon_{yy}^{(0)} \\ \gamma_{xy}^{(0)} \end{Bmatrix} + z \begin{Bmatrix} \epsilon_{xx}^{(1)} \\ \epsilon_{yy}^{(1)} \\ \gamma_{xy}^{(1)} \end{Bmatrix} + z^3 \begin{Bmatrix} \epsilon_{xx}^{(3)} \\ \epsilon_{yy}^{(3)} \\ \gamma_{xy}^{(3)} \end{Bmatrix} \quad (8 a)$$

$$\begin{Bmatrix} \gamma_{yz} \\ \gamma_{xz} \end{Bmatrix} = \begin{Bmatrix} \gamma_{yz}^{(0)} \\ \gamma_{xz}^{(0)} \end{Bmatrix} + z \begin{Bmatrix} \gamma_{yz}^{(1)} \\ \gamma_{xz}^{(1)} \end{Bmatrix} + z^3 \begin{Bmatrix} \gamma_{yz}^{(3)} \\ \gamma_{xz}^{(3)} \end{Bmatrix} \quad (8 b)$$

Where:

$$\begin{Bmatrix} \epsilon_{xx}^{(0)} \\ \epsilon_{yy}^{(0)} \\ \gamma_{yz}^{(0)} \\ \gamma_{xz}^{(0)} \\ \gamma_{xy}^{(0)} \end{Bmatrix} = \begin{Bmatrix} \frac{\partial u_0}{\partial x} - \alpha_x T_0 \\ \frac{\partial v_0}{\partial y} - \alpha_y T_0 \\ \frac{\partial w_0}{\partial y} + \phi_y \\ \frac{\partial w_0}{\partial x} + \phi_x \\ \frac{\partial u_0}{\partial y} + \frac{\partial v_0}{\partial x} - \alpha_{xy} T_0 \end{Bmatrix} \quad (8 c)$$

$$\begin{Bmatrix} \epsilon_{xx}^{(1)} \\ \epsilon_{yy}^{(1)} \\ \gamma_{yz}^{(1)} \\ \gamma_{xz}^{(1)} \\ \gamma_{xy}^{(1)} \end{Bmatrix} = \begin{Bmatrix} \frac{\partial \phi_x}{\partial x} - \alpha_x T_1 \\ \frac{\partial \phi_y}{\partial y} - \alpha_y T_1 \\ 0 \\ 0 \\ \frac{\partial \phi_x}{\partial y} + \frac{\partial \phi_y}{\partial x} - \alpha_{xy} T_1 \end{Bmatrix} \quad (8 d)$$

$$\begin{Bmatrix} \gamma_{yz}^{(2)} \\ \gamma_{xz}^{(2)} \end{Bmatrix} = -\frac{4}{h^2} \begin{Bmatrix} \frac{\partial w_0}{\partial y} + \phi_y \\ \frac{\partial w_0}{\partial x} + \phi_x \end{Bmatrix} \quad (8 e)$$

$$\begin{Bmatrix} \epsilon_{xx}^{(3)} \\ \epsilon_{yy}^{(3)} \\ \gamma_{xy}^{(3)} \end{Bmatrix} = -\frac{4}{3h^2} \begin{Bmatrix} \frac{\partial \phi_x}{\partial x} + \frac{\partial^2 w_0}{\partial x^2} \\ \frac{\partial \phi_y}{\partial y} + \frac{\partial^2 w_0}{\partial y^2} \\ \frac{\partial \phi_x}{\partial y} + \frac{\partial \phi_y}{\partial x} + 2 \frac{\partial^2 w_0}{\partial x \partial y} \end{Bmatrix} \quad (8 f)$$

The transformed stress-strain relations of an orthotropic lamina in are:

$$\begin{Bmatrix} \sigma_x \\ \sigma_y \\ \sigma_{xy} \end{Bmatrix}_k = \begin{bmatrix} \bar{Q}_{11} & \bar{Q}_{12} & \bar{Q}_{16} \\ \bar{Q}_{12} & \bar{Q}_{22} & \bar{Q}_{26} \\ \bar{Q}_{16} & \bar{Q}_{26} & \bar{Q}_{66} \end{bmatrix}_k \begin{Bmatrix} \epsilon_{xx} - \alpha_x \Delta T \\ \epsilon_{yy} - \alpha_y \Delta T \\ \gamma_{xy} - 2\alpha_{xy} \Delta T \end{Bmatrix} \quad (9 a)$$

$$\begin{Bmatrix} \sigma_{yz} \\ \sigma_{xz} \end{Bmatrix}_k = \begin{bmatrix} \bar{Q}_{44} & \bar{Q}_{45} \\ \bar{Q}_{45} & \bar{Q}_{55} \end{bmatrix}_k \begin{Bmatrix} \gamma_{yz} \\ \gamma_{xz} \end{Bmatrix} \quad (9 b)$$

Equation of Motion

The Euler-Lagrange equations are obtained by setting the coefficient of δu_0 , δv_0 , δw_0 , $\delta \phi_x$, $\delta \phi_y$ to zero separately [29]:

$$\delta u_0: \frac{\partial N_{xx}}{\partial x} + \frac{\partial N_{xy}}{\partial y} = 0 \quad (10 a)$$

$$\delta v_0 : \frac{\partial N_{xy}}{\partial x} + \frac{\partial N_{yx}}{\partial y} = 0 \quad (10 \text{ b})$$

$$\delta W_0 : \frac{\partial Q_x}{\partial x} - c_2 \frac{\partial R_x}{\partial x} + \frac{\partial Q_y}{\partial y} - c_2 \frac{\partial R_y}{\partial y} + c_1 \left(\frac{\partial^2 F_{xx}}{\partial x^2} + 2 \frac{\partial^2 F_{xy}}{\partial x \partial y} + \frac{\partial^2 F_{yy}}{\partial y^2} \right) + \hat{N}_{xx} \frac{\partial^2 w}{\partial x^2} + \hat{N}_{yy} \frac{\partial^2 w}{\partial y^2} + 2 \hat{N}_{xy} \frac{\partial^2 w}{\partial x \partial y} = 0 \quad (10 \text{ c})$$

$$\delta \Phi_x : \frac{\partial M_{xx}}{\partial x} - c_1 \frac{\partial F_{xx}}{\partial x} + \frac{\partial M_{xy}}{\partial y} - c_1 \frac{\partial F_{xy}}{\partial y} - Q_x + c_2 R_x = 0 \quad (10 \text{ d})$$

$$\delta \Phi_y : \frac{\partial M_{xy}}{\partial x} - c_1 \frac{\partial F_{xy}}{\partial x} + \frac{\partial M_{yy}}{\partial y} - c_1 \frac{\partial F_{yy}}{\partial y} - Q_y + c_2 R_y = 0 \quad (10 \text{ e})$$

Navier Method

Navier method can be used to solve the governing equations of various laminated plates for which when all four edges of the laminate are simply supported.

For cross-ply rectangular laminates with edges y=0 and y=b simply supported and the other two edges x=0 and x=a simply supported. Assume the following representation of the displacement:

$$u_0(x,y,t) = \sum_{n=1}^{\infty} \sum_{m=1}^{\infty} U_{mn}(t) \cos \alpha x \sin \beta y \quad (11 \text{ a})$$

$$v_0(x,y,t) = \sum_{n=1}^{\infty} \sum_{m=1}^{\infty} V_{mn}(t) \sin \alpha x \cos \beta y \quad (11 \text{ b})$$

$$w_0(x,y,t) = \sum_{n=1}^{\infty} \sum_{m=1}^{\infty} W_{mn}(t) \sin \alpha x \sin \beta y \quad (11 \text{ c})$$

$$\Phi_x(x,y,t) = \sum_{n=1}^{\infty} \sum_{m=1}^{\infty} X_{mn}(t) \cos \alpha x \sin \beta y \quad (11 \text{ d})$$

$$\Phi_y(x,y,t) = \sum_{n=1}^{\infty} \sum_{m=1}^{\infty} Y_{mn}(t) \sin \alpha x \cos \beta y \quad (11 \text{ e})$$

Where: $\alpha = \frac{m\pi}{a}$; $\beta = \frac{n\pi}{b}$

m = No. of half wavelengths in x-direction (m=1, 2, 3)

n = No. of half wavelengths in y-direction (n=1, 2, 3)

U_{mn} , V_{mn} , W_{mn} are arbitrary constants to be determined;

For angle-ply rectangular laminates with edges y=0 and y=b simply supported and the other two edges x=0 and x=a simply supported. Assume the following representation of the displacement [17]:

$$u_0(x,y,t) = \sum_{n=1}^{\infty} \sum_{m=1}^{\infty} U_{mn}(t) \sin \alpha x \cos \beta y \quad (12 \text{ a})$$

$$v_0(x,y,t) = \sum_{n=1}^{\infty} \sum_{m=1}^{\infty} V_{mn}(t) \cos \alpha x \sin \beta y \quad (12 \text{ b})$$

$$w_0(x,y,t) = \sum_{n=1}^{\infty} \sum_{m=1}^{\infty} W_{mn}(t) \sin \alpha x \sin \beta y \quad (12 \text{ c})$$

$$\Phi_x(x,y,t) = \sum_{n=1}^{\infty} \sum_{m=1}^{\infty} X_{mn}(t) \cos \alpha x \sin \beta y \quad (12 \text{ d})$$

$$w_y(x,y,t) = \sum_{n=1}^{\infty} \sum_{m=1}^{\infty} Y_{mn}(t) \sin \alpha x \cos \beta y \quad (12 e)$$

C. Finite Element Method

Finite element method has been employed to analyze critical buckling load for different boundary conditions and various laminate stacking sequences, aspect ratio, thickness ratio and for different number of layers. Analyses performed are this design study utilized a finite element model of the plate. The model was developed in ANSYS 13.0 using the 900 quadrature elements. The global x coordinate is directed along the width of the plate, while the global y coordinate is directed along the length and the global z direction corresponds to the thickness direction and taken to be the outward normal of the plate surface. There are 30 elements in the axial direction and 30 along the width (i.e. 16926 DOF). A convergence study has been performed to select the particular mesh used in this study. A linear buckling analysis (eigenvalue buckling) was performed on the model to calculate the minimum buckling load of the structure. The finite element model is described via an input file using APDL ANSYS language with SHELL 281. This element is suitable for analyzing thin to moderately thick shell structures. The element has eight nodes with six degrees of freedom at each node: translations in the x, y, and z axes, and rotations about the x, y, and z axes. It may be used for layered applications for modeling composite shells. It includes the effects of transverse shear deformation. The accuracy in modeling composite shells is

governed by the first order shear deformation theory.

Applying Load

It can be applied mechanical load on the solid model through lines. The solver expects all loads to be in terms of the finite element model. Therefore, the program automatically transfers all applied loads to the nodes and elements at the beginning of the solution.

For thermal load, the locations for temperature load is usually at the top and bottom planes called “pseudo-nodes” as shown in Fig. (1):

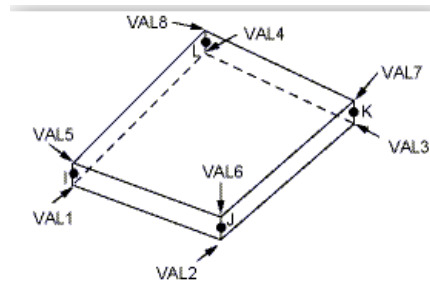


Fig. (1): thermal Load locations

Defining the Layer Configuration

The most important characteristic of a composite material is its layered configuration. Each layer may be made of a different orthotropic material and may have its principal directions oriented differently. For laminated composites, the fiber directions determine the layer orientation. The layer configuration is defined layer-by-layer from bottom to



top. The bottom layer is designed as layer 1, and additional layers are stacked from bottom to top in the positive Z (normal) direction of the element coordinate system. It can define layered sections via the section commands and the following properties are specified:

- Material properties.
- Layer orientation angle.
- Layer thickness.

Mesh Convergence

A convergence study was performed to determine the appropriate finite element mesh to be used in the linear buckling analysis of laminated plate model. Three meshes were developed, with increasing numbers of elements in the x and y directions.

The buckling loads for each of these models are shown in table (1). There is only a 0.7% difference between the load calculated for mesh 1 (7*7) and mesh 2 (15*15). A smaller difference (0.01 %) is observed between mesh 2 and mesh 3 (30*30). This indicates that the coarsest mesh is capable of performing the analysis within a reasonable degree of accuracy.

Table (1): Critical buckling load convergence study for C-C-S-C laminates

No.of Elements	No.of Nodes	No.of DOF	Critical buckling load $N_{xx}(N/m)$
49	176	1056	10452
225	736	4416	10379
900	2821	16926	10378

Computer Programming

The main computer program has been built for Levy method and Navier method to carry out the analysis required for solving the effect of mechanical and thermal loads on buckling analysis of composite laminated plate using classical and higher order shear deformation plate theory. However they involved complex calculations that are difficult to interpret physically and require considerably more computational effort. A computer code written in MATLAB (R2010a) consisting from 1400 steps approximately. This program has the following features. See Fig. (2):

1. It can solve a problem for (square, rectangular) composite laminated plate when two opposite edges are simply supported and other two edges any boundary conditions.
2. It can solve thin and thick laminated plate with any number of layers.
3. It can solve symmetric and anti-symmetric cross-ply and angle-ply composite laminated plate.
4. It can solve for critical mechanical load and critical thermal load that cause buckling and combination of these loads.

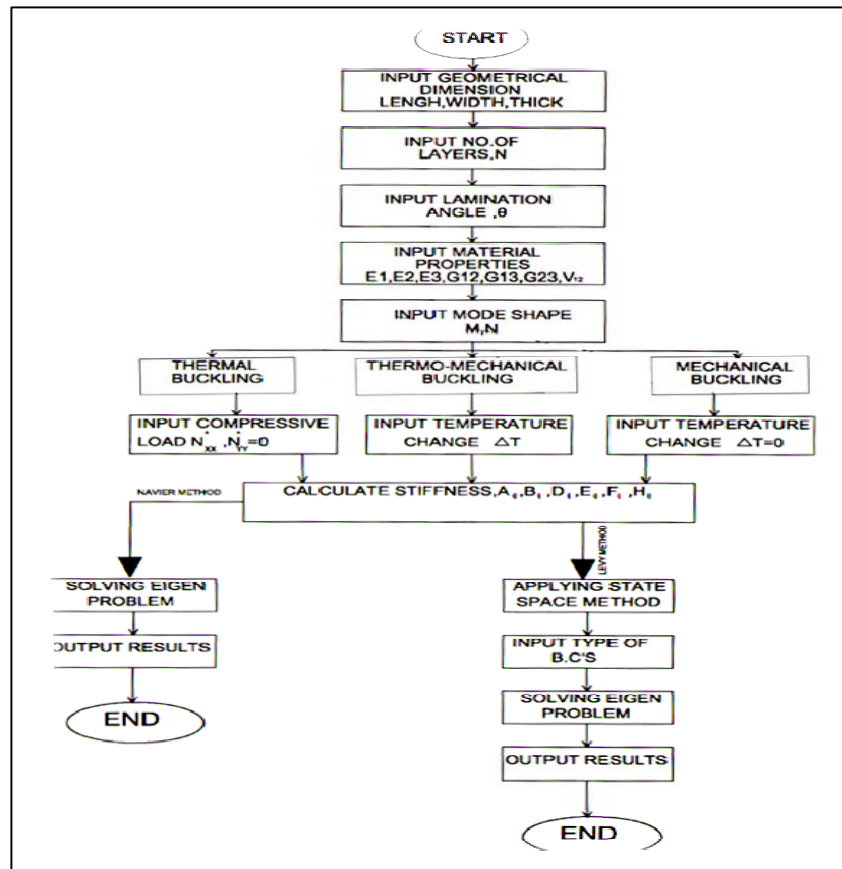


Fig. (2): MATLAB diagram

Verification Of Computer Program

In the present study, various combinations of edge support conditions have been investigated. For example, C-S-C-S means clamped edges at $x = (0, a)$ while simply supported at edges at $y = (0, b)$. To validate the present methods, thermo-mechanical buckling analysis of different boundary conditions laminated plates, the critical buckling load (thermal, mechanical) are plotted and compared below with [9], [15], and [17] as shown below. The results are compared to analytical solution (Levy and Navier) and numerical solution (Finite element method), the max. discrepancy in Fig.(3) was 4.195% when $b/h=100$ because [9]

used analytical solution (Navier method) without include membrane stiffness (that cause large deformation) while the present study include both membrane and bending stiffness.

Table (2): Dimensionless thermal buckling of square laminated plates $\bar{T} = T_{cr} \alpha_0 * 1000$

b/h	laminate	B.C'S	[15] (F.E)	ANSYS 13.0 (Discrepancy %)	
30	(45/-45) _{2T}	S-S-S-S	1.133	1.131 (0.1765%)	$E2/E1=0.081$ $G12=G13=0.031 E1$
50	(45/-45) _{2T}	S-S-S-S	0.443	0.44101 (3.0747%)	$G23=0.0304 E1$ $\nu12=0.21$ $\alpha1=-0.21 \alpha0$ $\alpha2=16 \alpha0$ $\alpha0=1e-6$

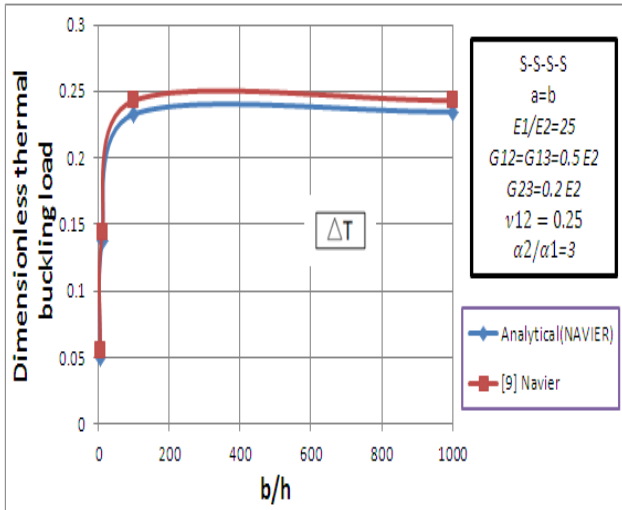


Fig.(3): Dimensionless critical temperature $\bar{T} = T_{cr} \frac{\alpha^2 h}{D_{22} \pi^2}$ of symmetric cross-ply 0/90/90/0 laminated plate

Table. (3): Dimensionless uniaxial buckling load $\bar{N} = N_{xx}^0 \frac{\alpha^2}{E_2 h^3}$ of anti-symmetric cross-ply laminates

B.C'S	b/h	[17] Levy	Present Levy (Discrepancy %)	Present Navier (Discrepancy %)	
S-F-S-F	50	16.426	17.53375 (6.3178%)	-	
S-F-S-S	50	17.023	18.11575 (6.032%)	-	
S-F-S-C	50	19.389	20.46825 (5.272%)	-	
S-S-S-S	50	35.232	36.351 (3.078%)	-	E1/E2=40
S-S-S-C	50	59.288	60.409 (1.855%)	-	G12=G13=0.6 E2
S-C-S-C	50	89.770	94.216 (4.718%)	-	G23=0.5 E2
S-S-S-S	5	12.109	-	13.0991 (7.558%)	nu12=0.25
S-S-S-S	10	25.423	-	24.8047 (2.432%)	a=b
					h=1
					N=10

From the above results, it is obvious that the methods of solution give reasonable results for both thermal and mechanical loads respectively.

Results And Discussions

A. Experimental Analysis

In view of difficulty of theoretical analysis of laminated structure behavior, experimental methods have become important in solving the buckling problem of laminated composite plates. In the present work, mechanical properties (Tensile test) and compressive behavior (buckling test) of (0/90/90/0) E-glass polyester laminated composite plates are calculated experimentally at room temperature.

Tensile Test

Each laminate was oriented in longitudinal, transverse and 45° angle relative to designated 0° direction to determine the engineering parameters E_1 , E_2 , G_{12} according to ASTM (D 638). The mechanical properties for glass-polyester are obtained from tensile test as shown in table (4).

Table (4): Experimental mechanical properties of Fiber glass-Polyester

Mechanical properties	Glass-polyester
E_1 (Mpa)	2473.046067
E_2 (Mpa)	1917.178
G_{12} (Mpa)	336
ν_{12} [10]	0.25
V_f	0.36

Buckling Test

In this study, buckling load of laminated plate determined analytically, numerically and experimentally. The laminated plate length was 220 mm. The width and thickness are 110 mm and 5.2 mm respectively. The specimen was loaded in axial compression (vertical direction) using tensile test machine of 100 KN capacities. The specimen was simply supported at two ends and kept free at the other two ends. The specimen was loaded slowly until buckling. Simply supported boundary conditions were simulated along the top and bottom edges. For axial loading, the test specimen was placed between two extremely stiff machine heads of which the lower one was fixed during the test, whereas the upper head was moved downwards by servo hydraulic cylinder. The laminated plate was loaded at constant cross-head speed of 2 mm/min.

The buckling load is determined from the load-displacement curve. The vertical displacement is plotted on the x-axis and load was plotted on the y-axis as shown in Fig. (4 a). For the determination of buckling load, the point where left from the straight line is determined on the graphics and the value of this point on the y-axis is called as the buckling load. The specimen was loaded in axial compression (vertical direction) using tensile test machine of 100 KN capacities as shown in Fig. (4 b). The specimen was simply supported at two ends and kept free at the other two ends. The specimen was loaded slowly until buckling.

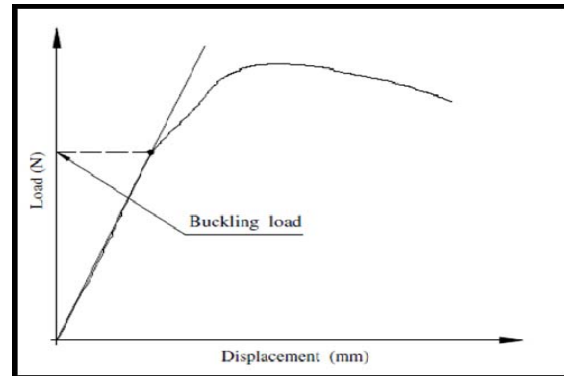


Fig. (4 a): The determination of buckling load



Fig. (4 b): Buckling test of F-S-F-S laminates

The agreement between the three methods was generally good. The max. discrepancy was 9.13% because there were bubbles and fiber glass is not straight in some portions. The critical buckling load is shown in table (5).

Table (5): Dimensionless buckling load [$\bar{N} = N_{yy}^0 * b^2 / E_2 * h^3$] of F-S-F-S laminates

Laminated plate	Length b (mm)	Width a (mm)	Thick. (mm)	Levy (Discrepancy%)	Finite element (Discrepancy%)	Experimental
(0/90) _s	220	110	5.2	3.4578 (7.89%)	3.4113 (9.13%)	3.75408

B. Theoretical Analysis

The present study focused mainly on the buckling behavior of composite laminated plates subjected to thermal (uniform, linear)(see eq. 6 a and 6 b) , mechanical and thermo-mechanical loads are analyzed by analytically and numerically for different aspect ratio, thickness ratio, lamination angle and number of layers with various boundary conditions and type of load (biaxial and uniaxial).

In present work, mechanical properties for glass-polyester are obtained from experimental results as shown in table (6).

Table. (6): Experimental mechanical properties of Fiber glass-Polyester

Mechanical properties	Glass-polyester
E_1 (GPa)	6.981
$E_2 = E_3$ (GPa)	2.0566
$G_{12} = G_{13}$	0.8979
$G_{13}=G_{23}$ (GPa)(assume)	0.8979
ν_{12} [9]	0.28
α_{xx} ($1/C^\circ$) [18]	$8.6 \alpha_0$
α_{yy} ($1/C^\circ$) [18]	$22.1 \alpha_0$
α_0 ($1/C^\circ$)	10^{-6}
V_f	0.34

1. Laminated Plate Subjected To Uniaxial Load Along Y-Axis

From Fig. (5), it can be shown that the buckling load is decrease in cases F-S-S-S and F-S-C-S because the effect of B.C'S. The buckling load is decreased with high percentage in F-S-C-S when a/b varies from 0.5 to 1. On other hand, this percentage gets smaller in F-S-S-S; F-S-C-S when a/b varies from 1 to 2.

In case F-S-F-S, the buckling load increase with small percentage when a/b varies from 0.5 to 2 because of its boundary condition.

It is worth mentioning that the decrease in buckling load in F-S-C-S is more than other case where this decrease reaches to 74.688% because the boundary effects on the middle region of the laminated plate decreases and consequently, the buckling load decreases.

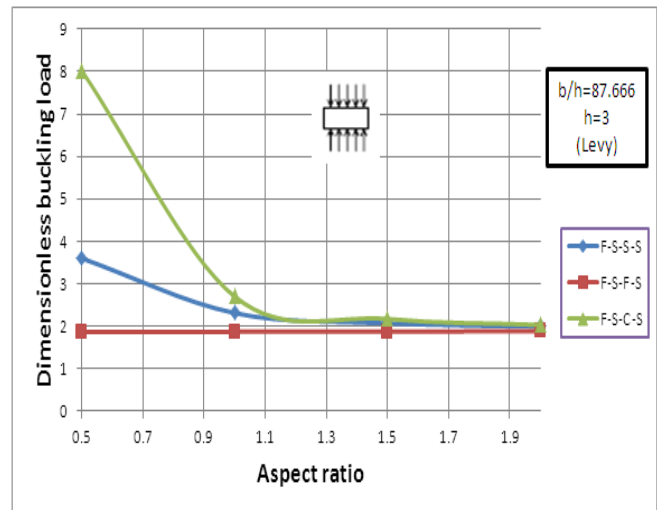


Fig. (5): Dimensionless uniaxial buckling load [$\bar{N} = N_{yy} * b^2 / E_2 * h^3$] versus aspect ratio , (a/b) of an anti-symmetric cross-ply $(0/90/0/90)_T$ laminates

In Fig.(6), the buckling load decrease when b/h varies from 10 to 50. The max. percentage of decreasing in buckling load occurs when b/h varies from 10 to 20 where this decrease reaches to 51.876 % because the effects of boundary on the middle region of the laminated plate diminish. So that, the buckling load encounters a significant decrease.

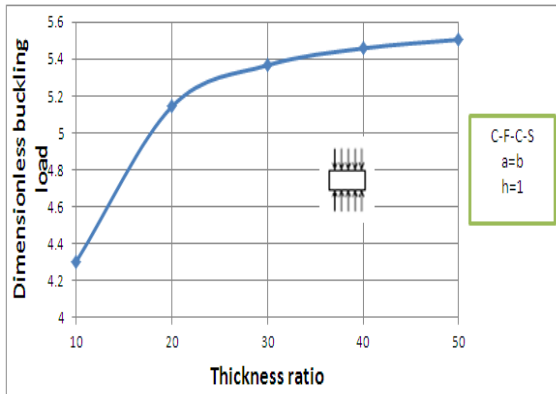


Fig. (6): Dimensionless uniaxial buckling load [$\bar{N} = N_{yy}^0 * b^2 / E_2 * h^3$] versus thickness ratio, (a/h) of an antisymmetric cross-ply $(0/90/0/90)_T$ laminates

Figs. (7) and (8) below shows the deformation of laminated plate at critical buckling load and it's deflection at first mode.

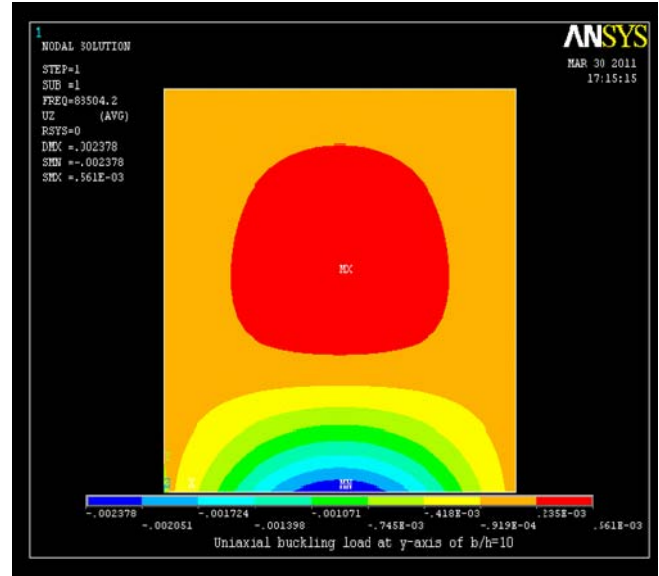


Fig. (8): Deflection of laminated plate for mode 1

2. Laminated Plate Subjected To Biaxial Load

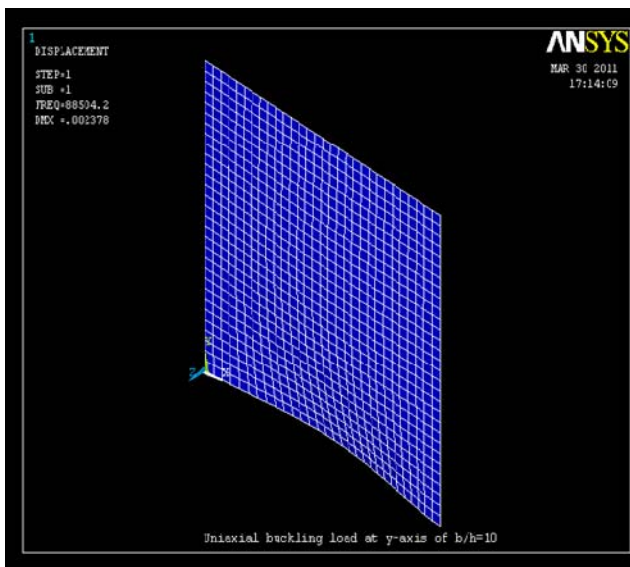


Fig. (7): Deformed shape of laminated plate for mode 1

From Fig.(9) , it can be obtained that biaxial load increase with high percentage when N varies from 2 to 4 because of the resistance of layers(that increase with increase the no. of layers) against load that cause buckling. Then, it will increase with small percentage when N varies from 4 to 10. Increasing in buckling load in case $(0/90)_T$ is more than other case, it reaches to 16.65%. The buckling load increase asymptotically when No. of layers increase.

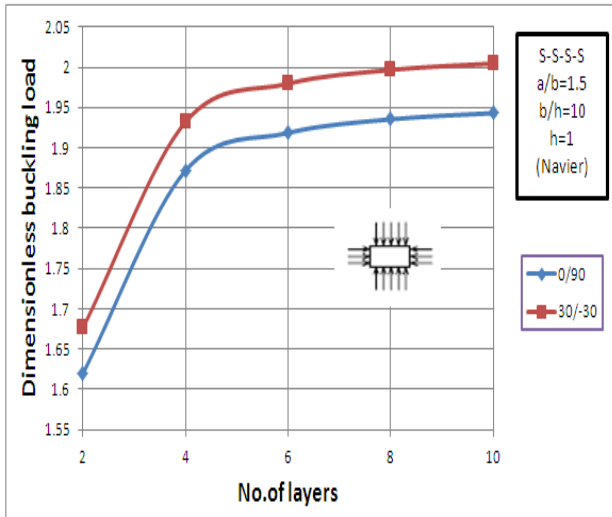


Fig. (9): Dimensionless Biaxial buckling load $[\bar{N} = N_{cr} * b^2 / E_2 * h^3]$ versus No. of layer for antisymmetric laminates

From Fig.(10), the buckling load decrease when a/b varies from 0.5 to 2. The max. percentage of decreasing in buckling load occurs when a/b varies from 0.5 to 1 where this decrease reaches to 52.626%.

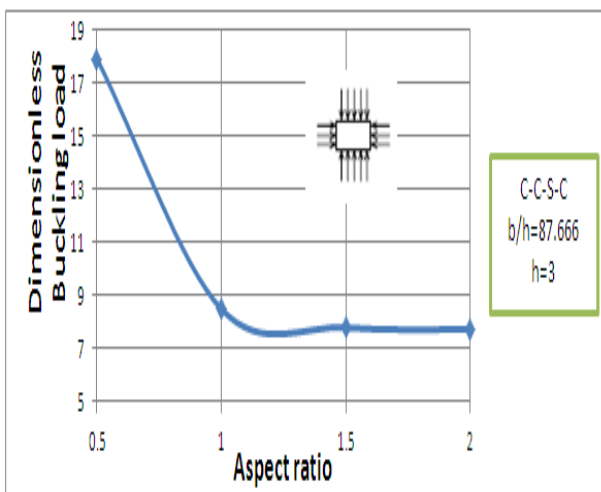


Fig. (10): Dimensionless biaxial buckling load $[\bar{N} = N_{cr} * b^2 / E_2 * h^3]$ versus aspect ratio , (a/b) of an antisymmetric cross-ply $(0/90/0/90)_T$ laminates

Figs. (11) and (12) below shows the deformation of laminated plate at critical buckling load and it's deflection at first mode.

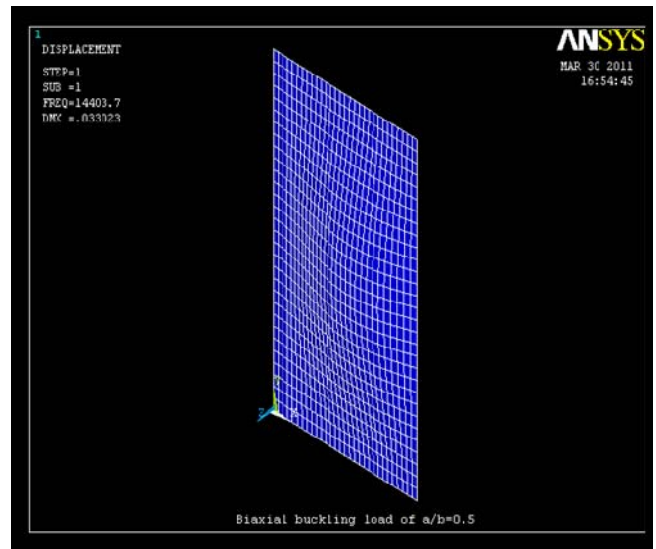


Fig. (11): Deformed shape of laminated plate for mode 1

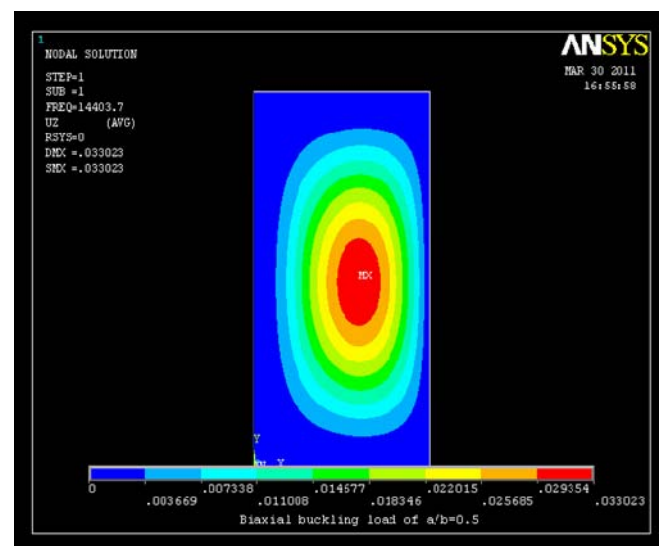


Fig. (12): Deflection of laminated plate for mode 1

Fig (13) shows the min. buckling load is shown when the value of half wavelengths is to be 2. Since the nearest integer value of n to critical buckling is to be when n is to be 3, then saying the right value of critical buckling load is to be when n=3.

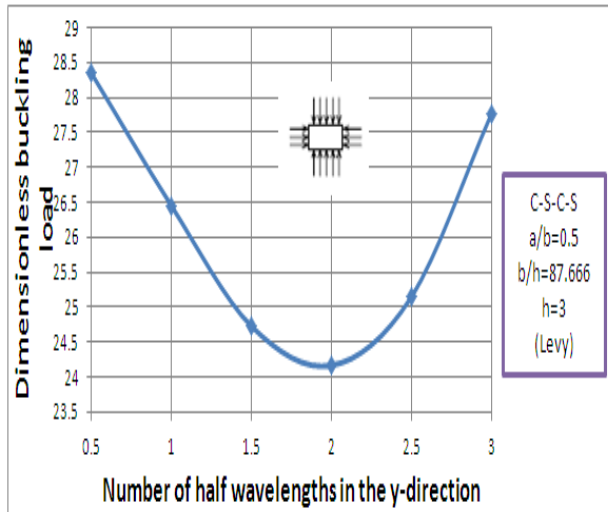


Fig. (13): Dimensionless Biaxial buckling load $[\bar{N} = N_{cr} * b^2 / E_2 * h^3]$ versus Number of half wavelengths in the y-direction , n of an antisymmetric cross-ply $(0/90/0/90)_T$ laminates

3. Laminated Plate Subjected To Uniaxial Load Along X-Axis

From Fig (14), it should be noted that the buckling load decrease with small percentage when θ varies because of the effect of B.C'S, while in case S-F-S-F it becomes to decrease higher when θ varies. The decrease in buckling load in S-F-S-F is more than other cases where this decrease reaches to 69.26%. On other hand, the min. percentage of

decreasing in buckling load is to be in S-C-S-F, it reaches to 46.532%.

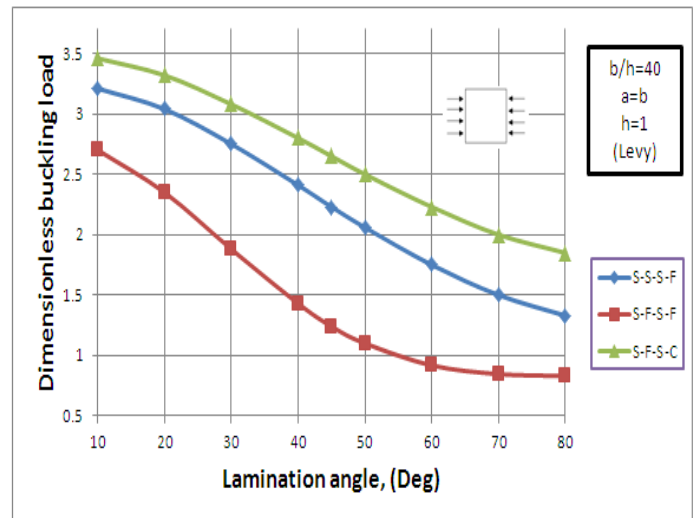


Fig. (14): Dimensionless uniaxial buckling load $[\bar{N} = N_{xxx}^0 * b^2 / E_2 * h^3]$ versus lamination angle , (θ) of an antisymmetric angle-ply $(\theta/-\theta/\theta/-\theta)$ laminates

4. Laminated Plate Subjected To Thermal Load

In the Fig.(15), it can be obtained that the buckling load is decrease with high percentage when a/b varies from 0.5 to 1. On other hand, this percentage get smaller when a/b varies from 1 to 2.

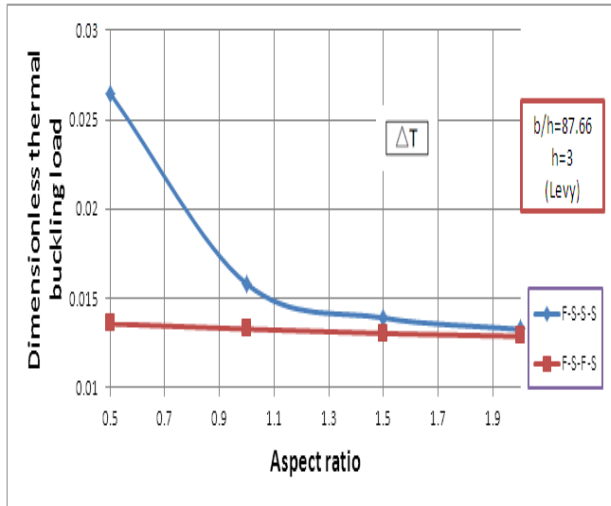


Fig. (15): Dimensionless Linear Thermal buckling load [$\bar{T} = T_{cr} * \alpha_0 * 1000$] versus aspect ratio , (a/b) of an antisymmetric cross-ply $(0/90/0/90)_S$ laminates

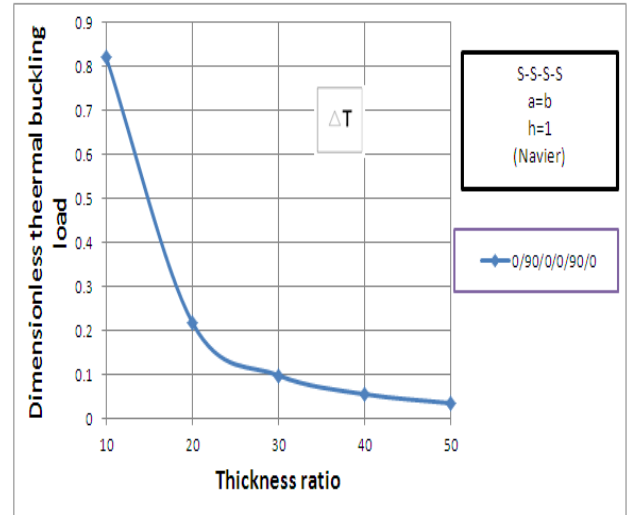


Fig. (16): Dimensionless Uniform Thermal buckling load [$\bar{T} = T_{cr} * \alpha_0 * 1000$] versus thickness ratio , (a/h) laminates

Fig.(16) shows that the buckling load was decrease with high percentage when b/h varies from 10 to 20 because the total thickness was decrease Then this percentage gets smaller when b/h varies from 20 to 50.

5. Laminated Plate Subjected To Thermo-Mechanical Load

The uniaxial buckling load for different cases is summarized. It is important to note that the max. buckling load decreases with different percentage when T increase.

In table (7), deals with thick laminated plate; the decrease in buckling load in case $(0/90)_S$ is more than other cases because $(0/90)_S$ of laminated rectangular plate is less stiffness than other cases; this decrease reaches to 12.5% but the decrease in buckling load in $(45/-45/45/-45/45)_T$ is less than other cases, it reaches to 8.15%.

Table. (7): Dimensionless uniaxial buckling load [$\bar{N} = N_{xx}^0 * b^2 / E_2 * h^3$] of laminated plates under uniformly temperature distribution

Lamination Scheme	Boundary condition	a/b	b/h	Buckling load (Navier)			
				$\Delta T=0^\circ\text{C}$	$\Delta T=20^\circ\text{C}$	$\Delta T=40^\circ\text{C}$	$\Delta T=60^\circ\text{C}$
$(0/90)_s$	S-S-S-S	1.5	10	5.1532	4.8953	4.7	4.5049
$(0/90/90/0/0)_s$	S-S-S-S	1.5	10	6.1228	5.9302	5.7376	5.545
$(0/90)_T$	S-S-S-S	1.5	10	6.079	5.8245	5.6292	5.434
$(0/90/90/0/0)_T$	S-S-S-S	1.5	10	5.7163	5.5237	5.3312	5.1386
$(45/-45)_T$	S-S-S-S	1.5	10	7.29	7.0542	6.859	6.6638
$(45/-45/45/-45/45)_T$	S-S-S-S	1.5	10	7.6185	7.3875	7.1923	6.997

From Fig.(17), it can be obtained that the buckling load is decrease with small percentage when temperature varies from 0°C to 30°C where the percentage decreases in buckling load reaches to 10.25% along temperature variations.

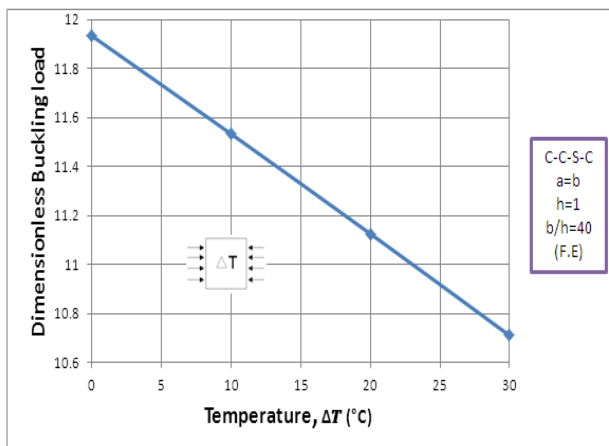


Fig. (17): Dimensionless uniaxial buckling load [$\bar{N} = N_{xx}^0 * b^2 / E_2 * h^3$] versus temperature varying linearly of symmetric angle-ply $(30/-30)_s$ laminates

Figs. (18) and (19) below shows the deformation of laminated plate at critical buckling load and it's deflection at first mode.

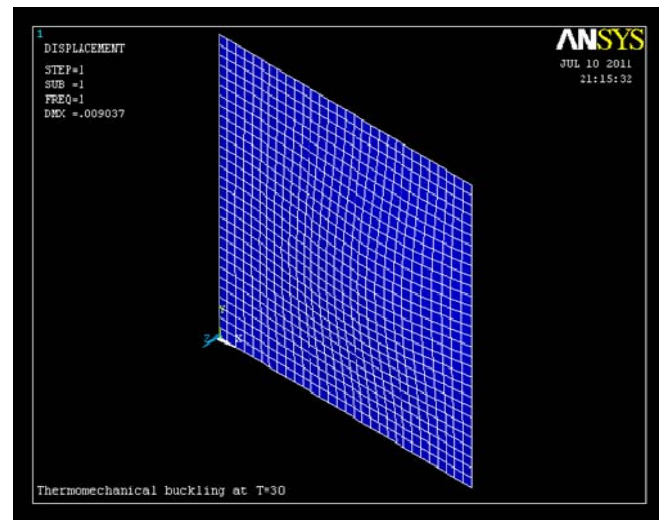


Fig. (18): Deformed shape of laminated plate for mode 1

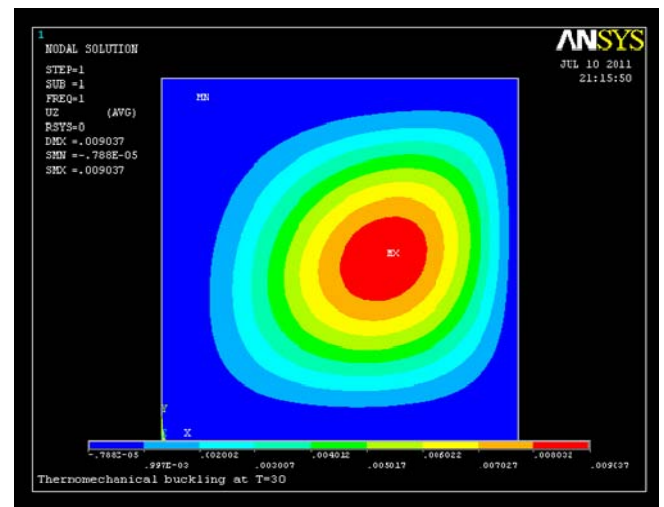


Fig. (19): Deflection of laminated plate for mode 1



Conclusion

This study considers the buckling analysis of cross-ply and angle-ply laminates with various B.C's. From the present analytical study, the following conclusions can be made:

1. It was noted that different thickness ratio affected the critical buckling load. The buckling load decrease when b/h increase and reaches to min. value at b/h=50. The max. decrease in buckling load occurs when b/h varies from 10 to 20.
2. As the aspect ratio increases, the critical buckling load of laminated plate decreases and reaches to min. value at a/b=2. The max. decrease in buckling load occurs when a/b varies from 0.5 to 1.
3. It was seen that the different fiber orientation angles affected the critical buckling load. When the fiber angle increases, the buckling load decreases and reaches to min. value at $\theta=80$,
4. It is clear that No. of layers affected on critical buckling load. The buckling load increase when No. of layers increase and reaches to max. value at N=10. The max. increase in buckling load occurs when N varies from 2 to 4.
5. It was seen that No. of half wavelengths affected on buckling load because critical buckling load (the value of min.

load) may not occur in the first half wavelengths. It may lie in the second or third half wavelengths.

6. The boundary conditions affect the buckling load, the buckling load increase when boundary conditions become more stiffness.

Appendix A

Classical laminated plate theory

The in plane force resultants are defined as

$$\begin{pmatrix} N_{xx} \\ N_{yy} \\ N_{xy} \end{pmatrix} = \int_{-h/2}^{h/2} \begin{pmatrix} \sigma_x \\ \sigma_y \\ \sigma_{xy} \end{pmatrix}_k dz = \sum_{k=1}^N \int_{z_k}^{z_{k+1}} \begin{pmatrix} \sigma_x \\ \sigma_y \\ \sigma_{xy} \end{pmatrix}_k dz \quad (A-1)$$

Where σ_x , σ_y and τ_{xy} are normal and shear stress.

α_x , α_y and α_{xy} are thermal expansion coefficients

$$\begin{pmatrix} N_{xx} \\ N_{yy} \\ N_{xy} \end{pmatrix} = \begin{bmatrix} A_{11} & A_{12} & A_{16} \\ A_{12} & A_{22} & A_{26} \\ A_{16} & A_{26} & A_{66} \end{bmatrix} \begin{pmatrix} \epsilon_{xx}^0 \\ \epsilon_{yy}^0 \\ \gamma_{xy}^0 \end{pmatrix} + \begin{bmatrix} B_{11} & B_{12} & B_{16} \\ B_{12} & B_{22} & B_{26} \\ B_{16} & B_{26} & B_{66} \end{bmatrix} \begin{pmatrix} \epsilon_{xx}^1 \\ \epsilon_{yy}^1 \\ \gamma_{xy}^1 \end{pmatrix} - \begin{pmatrix} N_x^T \\ N_y^T \\ N_{xy}^T \end{pmatrix} \quad (A-2)$$

$$\begin{Bmatrix} M_{xx} \\ M_{yy} \\ M_{xy} \end{Bmatrix} = \int_{-h/2}^{h/2} \begin{Bmatrix} \sigma_x \\ \sigma_y \\ \sigma_{xy} \end{Bmatrix}_k dz = \sum_{k=1}^N \int_{z_k}^{z_{k+1}} \begin{Bmatrix} \sigma_x \\ \sigma_y \\ \sigma_{xy} \end{Bmatrix}_k z dz \quad (\text{A-3})$$

$$\begin{Bmatrix} M_{xx} \\ M_{yy} \\ M_{xy} \end{Bmatrix} = \begin{bmatrix} B_{11} & B_{12} & B_{16} \\ B_{12} & B_{22} & B_{26} \\ B_{16} & B_{26} & B_{66} \end{bmatrix} \begin{Bmatrix} \varepsilon_{xy}^0 \\ \varepsilon_{xy}^0 \\ \gamma_{xy}^0 \end{Bmatrix} + \begin{bmatrix} D_{11} & D_{12} & D_{16} \\ D_{12} & D_{22} & D_{26} \\ D_{16} & D_{26} & D_{66} \end{bmatrix} \begin{Bmatrix} \varepsilon_{xx}^1 \\ \varepsilon_{yy}^1 \\ \gamma_{xy}^1 \end{Bmatrix} - \begin{Bmatrix} M_x^T \\ M_y^T \\ M_{xy}^T \end{Bmatrix} \quad (\text{A-4})$$

Where $\{N^T\}$ and $\{M^T\}$ are thermal stress and bending results, respectively

$$\begin{Bmatrix} N_x^T, M_x^T \\ N_y^T, M_y^T \\ N_{xy}^T, M_{xy}^T \end{Bmatrix} = \sum_{k=1}^N \int_{-h/2}^{h/2} \begin{bmatrix} \bar{Q}_{11} & \bar{Q}_{12} & \bar{Q}_{16} \\ \bar{Q}_{12} & \bar{Q}_{22} & \bar{Q}_{26} \\ \bar{Q}_{16} & \bar{Q}_{26} & \bar{Q}_{66} \end{bmatrix} \begin{Bmatrix} \alpha_x \\ \alpha_y \\ 2\alpha_{xy} \end{Bmatrix} (1, z) \Delta T dz \quad (\text{A-5})$$

For uniform temperature variation:
 $\Delta T = \text{applied temperature} - \text{reference temperature}$ (A-6)

For linear temperature variation:
 $\Delta T = T_0(x, y, t) + z * T_1(x, y, t)$ (A-7)

Here, A_{ij} are the extensional stiffness, B_{ij} the coupling stiffness, and D_{ij} the bending stiffness.

$$A_{ij} = \sum_{k=1}^N (\bar{Q}_{ij})_k (z_{k+1} - z_k) \quad (\text{A-8})$$

$$B_{ij} = \frac{1}{2} \sum_{k=1}^N (\bar{Q}_{ij})_k (z_{k+1}^2 - z_k^2) \quad (\text{A-9})$$

$$D_{ij} = \frac{1}{3} \sum_{k=1}^N (\bar{Q}_{ij})_k (z_{k+1}^3 - z_k^3) \quad (\text{A-10})$$

Appendix B

Third order shear deformation plate theory

The in-plane force resultants are defined as:

$$\begin{Bmatrix} N_{xx} \\ N_{yy} \\ N_{xy} \end{Bmatrix} = \int_{-h/2}^{h/2} \begin{Bmatrix} \sigma_x \\ \sigma_y \\ \sigma_{xy} \end{Bmatrix}_k dz = \sum_{k=1}^N \int_{z_k}^{z_{k+1}} \begin{Bmatrix} \sigma_x \\ \sigma_y \\ \sigma_{xy} \end{Bmatrix}_k dz \quad (\text{B-1})$$

$$\begin{Bmatrix} N_{xx} \\ N_{yy} \\ N_{xy} \end{Bmatrix} = \begin{bmatrix} A_{11} & A_{12} & A_{16} \\ A_{12} & A_{22} & A_{26} \\ A_{16} & A_{26} & A_{66} \end{bmatrix} \begin{Bmatrix} \varepsilon_{xy}^0 \\ \varepsilon_{xy}^0 \\ \gamma_{xy}^0 \end{Bmatrix} + \begin{bmatrix} B_{11} & B_{12} & B_{16} \\ B_{12} & B_{22} & B_{26} \\ B_{16} & B_{26} & B_{66} \end{bmatrix} \begin{Bmatrix} \varepsilon_{xx}^1 \\ \varepsilon_{yy}^1 \\ \gamma_{xy}^1 \end{Bmatrix} - c_1 \begin{bmatrix} E_{11} & E_{12} & E_{16} \\ E_{12} & E_{22} & E_{26} \\ E_{16} & E_{26} & E_{66} \end{bmatrix} \begin{Bmatrix} \varepsilon_{xx}^{(3)} \\ \varepsilon_{yy}^{(3)} \\ \gamma_{xy}^{(3)} \end{Bmatrix} - \begin{Bmatrix} N_x^T \\ N_y^T \\ N_{xy}^T \end{Bmatrix} \quad (\text{B-2})$$

$$\begin{aligned} \begin{Bmatrix} M_{xx} \\ M_{yy} \\ M_{xy} \end{Bmatrix} &= \int_{-h/2}^{h/2} \begin{Bmatrix} \sigma_x \\ \sigma_y \\ \sigma_{xy} \end{Bmatrix}_k z dz = \\ \sum_{k=1}^N \int_{z_k}^{z_{k+1}} \begin{Bmatrix} \sigma_x \\ \sigma_y \\ \sigma_{xy} \end{Bmatrix}_k z dz \end{aligned} \tag{B-3}$$

$$\begin{aligned} \begin{Bmatrix} P_{xx} \\ P_{yy} \\ P_{xy} \end{Bmatrix} &= \begin{bmatrix} E_{11} & E_{12} & E_{16} \\ E_{12} & E_{22} & E_{26} \\ E_{16} & E_{26} & E_{66} \end{bmatrix} \begin{Bmatrix} \varepsilon_{xx}^0 \\ \varepsilon_{xy}^0 \\ \gamma_{xy}^0 \end{Bmatrix} + \\ \begin{bmatrix} F_{11} & F_{12} & F_{16} \\ F_{12} & F_{22} & F_{26} \\ F_{16} & F_{26} & F_{66} \end{bmatrix} \begin{Bmatrix} \varepsilon_{xx}^1 \\ \varepsilon_{yy}^1 \\ \gamma_{xy}^1 \end{Bmatrix} \end{aligned}$$

$$\begin{aligned} \begin{Bmatrix} M_{xx} \\ M_{yy} \\ M_{xy} \end{Bmatrix} &= \begin{bmatrix} B_{11} & B_{12} & B_{16} \\ B_{12} & B_{22} & B_{26} \\ B_{16} & B_{26} & B_{66} \end{bmatrix} \begin{Bmatrix} \varepsilon_{xy}^0 \\ \varepsilon_{xy}^0 \\ \gamma_{xy}^0 \end{Bmatrix} \\ + \begin{bmatrix} D_{11} & D_{12} & D_{16} \\ D_{12} & D_{22} & D_{26} \\ D_{16} & D_{26} & D_{66} \end{bmatrix} \begin{Bmatrix} \varepsilon_{xx}^1 \\ \varepsilon_{yy}^1 \\ \gamma_{xy}^1 \end{Bmatrix} \end{aligned}$$

$$\begin{aligned} c_1 \begin{bmatrix} H_{11} & H_{12} & H_{16} \\ H_{12} & H_{22} & H_{26} \\ H_{16} & H_{26} & H_{66} \end{bmatrix} \begin{Bmatrix} \varepsilon_{xx}^{(3)} \\ \varepsilon_{yy}^{(3)} \\ \gamma_{xy}^{(3)} \end{Bmatrix} \\ \begin{Bmatrix} P_x^T \\ P_y^T \\ P_{xy}^T \end{Bmatrix} \end{aligned} \tag{B-6}$$

$$\begin{aligned} c_1 \begin{bmatrix} F_{11} & F_{12} & F_{16} \\ F_{12} & F_{22} & F_{26} \\ F_{16} & F_{26} & F_{66} \end{bmatrix} \begin{Bmatrix} \varepsilon_{xx}^{(3)} \\ \varepsilon_{yy}^{(3)} \\ \gamma_{xy}^{(3)} \end{Bmatrix} \\ \begin{Bmatrix} M_x^T \\ M_y^T \\ M_{xy}^T \end{Bmatrix} \end{aligned} \tag{B-4}$$

$$\begin{aligned} \begin{Bmatrix} Q_{yz} \\ Q_{xz} \end{Bmatrix} &= \int_{-h/2}^{h/2} \begin{Bmatrix} \sigma_{yz} \\ \sigma_{xz} \end{Bmatrix}_k dz = \\ \sum_{k=1}^N \int_{z_k}^{z_{k+1}} \begin{Bmatrix} \sigma_{yz} \\ \sigma_{xz} \end{Bmatrix}_k dz \end{aligned} \tag{B-7}$$

$$\begin{aligned} \begin{Bmatrix} P_{xx} \\ P_{yy} \\ P_{xy} \end{Bmatrix} &= \int_{-h/2}^{h/2} \begin{Bmatrix} \sigma_x \\ \sigma_y \\ \sigma_{xy} \end{Bmatrix}_k z^2 dz = \\ \sum_{k=1}^N \int_{z_k}^{z_{k+1}} \begin{Bmatrix} \sigma_x \\ \sigma_y \\ \sigma_{xy} \end{Bmatrix}_k z^2 dz \end{aligned} \tag{B-5}$$

$$\begin{aligned} \begin{Bmatrix} Q_{yz} \\ Q_{xz} \end{Bmatrix} &= \begin{bmatrix} A_{44} & A_{45} \\ A_{45} & A_{55} \end{bmatrix} \begin{Bmatrix} \gamma_{yz}^{(0)} \\ \gamma_{xz}^{(0)} \end{Bmatrix} \\ c_2 \begin{bmatrix} D_{44} & D_{45} \\ D_{45} & D_{55} \end{bmatrix} \begin{Bmatrix} \gamma_{yz}^{(2)} \\ \gamma_{xz}^{(2)} \end{Bmatrix} \end{aligned} \tag{B-8}$$

$$\begin{aligned} \begin{Bmatrix} R_{yz} \\ R_{xz} \end{Bmatrix} &= \int_{-h/2}^{h/2} \begin{Bmatrix} \sigma_{yz} \\ \sigma_{xz} \end{Bmatrix}_k z^2 dz = \\ \sum_{k=1}^N \int_{z_k}^{z_{k+1}} \begin{Bmatrix} \tau_{yz} \\ \tau_{xz} \end{Bmatrix}_k z^2 dz \end{aligned} \tag{B-9}$$

$$\begin{aligned} \begin{Bmatrix} R_{yz} \\ R_{xz} \end{Bmatrix} &= \begin{bmatrix} D_{44} & D_{45} \\ D_{45} & D_{55} \end{bmatrix} \begin{Bmatrix} \gamma_{yz}^{(0)} \\ \gamma_{xz}^{(0)} \end{Bmatrix} \\ c_2 \begin{bmatrix} F_{44} & F_{45} \\ F_{45} & F_{55} \end{bmatrix} \begin{Bmatrix} \gamma_{yz}^{(2)} \\ \gamma_{xz}^{(2)} \end{Bmatrix} \end{aligned} \tag{B-10}$$

Where

$$A_{ij}, B_{ij}, D_{ij}, E_{ij}, F_{ij}, H_{ij} = \sum_{k=1}^N \int_{z_k}^{z_{k+1}} \bar{Q}_{ij}^{(k)} (1, z, z^2, z^3, z^4, z^5) dz \quad (\text{B-11})$$

Where $\{N^T\}$, $\{M^T\}$ and $\{P^T\}$ are thermal stress results

$$\left\{ \begin{matrix} N_x^T, M_x^T, P_x^T \\ N_y^T, M_y^T, P_y^T \\ N_{xy}^T, M_{xy}^T, P_{xy}^T \end{matrix} \right\} = \sum_{k=1}^N \int_{-h/2}^{h/2} \begin{bmatrix} \bar{Q}_{11} & \bar{Q}_{12} & \bar{Q}_{16} \\ \bar{Q}_{12} & \bar{Q}_{22} & \bar{Q}_{26} \\ \bar{Q}_{16} & \bar{Q}_{26} & \bar{Q}_{66} \end{bmatrix} \begin{Bmatrix} \alpha_x \\ \alpha_y \\ 2\alpha_{xy} \end{Bmatrix} (1, z, z^3) \Delta T dz \quad (\text{B-12})$$

References

Gossard M.L., Seide P., and Roberts W.M. “ **Thermal buckling of plates** “. NASA TN 2771; 1952.

Sharma S., Iyengar N.G.R., and Murthy P.N. “ **Buckling of anti-symmetric cross and angle-ply laminated plates** “. Int. J. Mech. Sci. 1980; 22: 607-620.

Thangaratnam K.R., Palaninathan, and Ramachandran J. “ **Thermal buckling of composite laminated plates** “. J computers and structures 1988; 32(5): 1117-1124.

Liangxin S. and Zhiyus S. “ **The analysis of laminated composite plates based on the simple higher order theory** “. J computers and structures 1992; 43(5): 831-837.

Kam T.Y. and Chang R.R. “ **Design of laminated composite plates for maximum buckling load and vibration frequency** “. J computer

methods in applied mechanics and engineering 1993; 106: 65-81.

Prabhu M.R. and Dhanaraj R. “ **Thermal buckling of laminated composite plates** “. J computers and structures 1994; 53(5): 1193-1204.

Argyris J. and Tenek L. “ **High-temperature bending, buckling and postbuckling of laminated composite plates using the natural mode method** “. J computer methods in applied mechanics and engineering 1994;117 :105-142.

Ghosh A.K. and Dey S.K. “ **Buckling of laminated plates – a simple finite element based on higher-order theory** “. J finite elements in analysis and design 1994; 15:289-302.

Sun L. and Xiaoping S. “ **Thermo-mechanical buckling of laminated composite plates with higher-order transverse shear deformation** “. J computers and structures 1994; 53(1): 1-7.

Simelane S. P. “ **Thermal buckling of laminated composite Plates**” . M.Sc thesis; South Africa; 1998.

Matsunaga H. “ **Thermal buckling of cross-ply laminated composite and sandwich plates according to a global higher-order deformation theory** “. J composite structures 2005; 68:439-454.

Shariyat M. “ **Thermal buckling analysis of rectangular composite plates with temperature-dependent properties based on a layerwise**



theory “. J thin-walled structures 2007; 45:439-452.

Yu L.H. and Wang C.Y. “ **Buckling of rectangular plates on an elastic foundation using the Levy method** “. J AIAA 2008; 46(12):3163-3166.

Ozben T. “ **Analysis of critical buckling load of laminated composites plate with different boundary conditions using FEM and analytical methods** “. J computational materials science 2009; 45:1006-1015.

Rajesh K., Lal A., and Singh B.N. “ **Effects of random system properties on the thermal buckling analysis of laminated composite plated** “. J computers and structures 2009; 87:1119-1128.

Shiau L., Kuo S., and Chen C. “ **Thermal buckling behavior of composite laminated plates** “. J composite structures 2010; 92: 508-514.

Reddy J.N. “ **Mechanics of laminated composite plates and shells: theory and analysis** “. 2ed; CRC Press 2004.

Zaffer G. “ **Design and optimization of laminated composite materials** “. Canada; John Wiley & Sons 1999.

Hasanain I. N. “ **Buckling analysis of composite plates under thermal and mechanical loading** “. M.Sc. thesis; University of Baghdad; 2011

Nomenclature

Symbol	Description	Units
a	Dimension along x-coordinate	m
b	Dimension along y-coordinate	m
$A_{ij}, B_{ij}, D_{ij}, E_{ij}, F_{ij}, H_{ij}$	Extensional, bending extensional coupling, bending and additional stiffness	-
E_1, E_2, E_3	Elastic modulus components	Gpa
G_{12}, G_{23}, G_{13}	Shear modulus components	Gpa
h	Thickness	m
m, n	No. of half wavelengths in x and y directions	-
N	Total number of plate layers	-

Symbol	Description	Units
N_{xx}, N_{yy}, N_{xy}	In-plane force resultant	N/m
M_{xx}, M_{yy}, M_{xy}	Moment resultant per unit length	N.m/m
P_{xx}, P_{yy}, P_{xy}	Resultant force per unit length	N/m
Q_{xz}, Q_{yz}	Transverse shear force resultant	N
R_{xz}, R_{yz}	Transverse shear force resultant (HSDT)	N
$\bar{Q}_{ij}^{(k)}$	Transformed lamina stiffness	N/m
z	Distance from neutral axis	m
x, y, z	Cartesian coordinate system	m
Z_k, Z_{k+1}	Upper and lower lamina surface coordinates along z-direction	m
$\alpha_{xx}, \alpha_{yy}, \alpha_{xy}$	Transformed thermal coefficients of expansion	$1/^\circ\text{C}$
$\epsilon_{xx}, \epsilon_{yy}, \epsilon_{xy}, \epsilon_{xz}, \epsilon_{yz}, \epsilon_{zz}$	Strain components	m/m
ΔT	Temperature increment	$^\circ\text{C}$
γ_{xz}, γ_{yz}	Transverse shear strain	m/m
ν_{12}	Poisson's ratio component	-



Symbol	Description	Units
$\sigma_{xx}, \sigma_{yy},$ σ_{xy}, σ_{xz} σ_{yz}	Stress components	Gpa
C-S-C-S	Clamped at x-axis and simply supported at y-axis	-
N_{xx}^T, N_{yy}^T	Thermal stress resultant	N/m
N_{xx}^0, N_{yy}^0	Applied edge forces	N/m
θ	Fiber orientation angle	Degree
$U_{mn}, V_{mn},$ $W_{mn},$ X_{mn}, Y_{mn}	Arbitrary constant	-
u, v, w u, v, w	Displacement component	M
T	Temperature	C^0
1, 2, 3	Principal material coordinate system	-
$(0/90)_S$	Symmetric cross-ply laminate	-
$(0/90)_T$	Anti Symmetric cross-ply laminate	-
$(\theta/-\theta)_T$	Anti symmetric angle-ply laminate	-
$(\theta/-\theta)_S$	Symmetric angle-ply laminate	-
S	Simply supported edge	-
C	Clamped edge	-`
F	Free edge	-

**Prof. Dr. Adnan Naji Jameel
Dr. Ibtehal Abbas Sadiq
Hasanain Ibraheem Nsaif**

**Buckling Analysis of Composite Plates under
Thermal and Mechanical Loading**